Cell Oncol. (2017) 40:549–561
DOI 10.1007/s13402-017-0343-7

ORIGINAL PAPER

Increased EGFR expression induced by a novel oncogene, CUG2, confers resistance to doxorubicin through Stat1-HDAC4 signaling

Sirichat Kaowinn[1] · Seung Won Jun[1] · Chang Seok Kim[1] · Dong-Myeong Shin[2] · Yoon-Hwae Hwang[2] · Kyujung Kim[3] · Bosung Shin[3] · Chutima Kaewpiboon[4] · Hyeon Hee Jeong[5] · Sang Seok Koh[5] · Oliver H. Krämer[6] · Randal N. Johnston[7] · Young-Hwa Chung[1]

Accepted: 26 July 2017 / Published online: 3 August 2017

Abstract

Background Previously, it has been found that the cancer upregulated gene 2 (CUG2) and the epidermal growth factor receptor (EGFR) both contribute to drug resistance of cancer cells. Here, we explored whether CUG2 may exert its anticancer drug resistance by increasing the expression of EGFR.

Methods EGFR expression was assessed using Western blotting, immunofluorescence and capacitance assays in A549 lung cancer and immortalized bronchial BEAS-2B cells, respectively, stably transfected with a CUG2 expression vector (A549-CUG2; BEAS-CUG2) or an empty control vector (A549-Vec; BEAS-Vec). After siRNA-mediated EGFR, Stat1 and HDAC4 silencing, antioxidant and multidrug resistance protein and mRNA levels were assessed using Western blotting and RT-PCR. In addition, the respective cells were treated with doxorubicin after which apoptosis and reactive oxygen species (ROS) levels were measured. Stat1 acetylation was assessed by immunoprecipitation.

Results We found that exogenous CUG2 overexpression induced EGFR upregulation in A549 and BEAS-2B cells, whereas EGFR silencing sensitized these cells to doxorubicin-induced apoptosis. In addition, we found that exogenous CUG2 overexpression reduced the formation of ROS during doxorubicin treatment by enhancing the expression of antioxidant and multidrug resistant proteins such as MnSOD, Foxo1, Foxo4, MRP2 and BCRP, whereas EGFR silencing congruently increased the levels of ROS by decreasing the expression of these proteins. We also found that EGFR silencing and its concomitant Akt, ERK, JNK and p38 MAPK inhibition resulted in a decreased Stat1 phosphorylation and, thus, a decreased activation. Since also acetylation can affect Stat1 activation via a phospho-acetyl switch, HDAC inhibition may sensitize cells to doxorubicin-induced apoptosis. Interestingly, we found that exogenous CUG2 overexpression upregulated HDAC4, but not HDAC2 or HDAC3. Conversely, we found that HDAC4 silencing sensitized the cells to doxorubicin resistance by decreasing Stat1 phosphorylation and EGFR expression, thus indicating an interplay between HDAC4, Stat1 and EGFR.

Conclusion Taken together, we conclude that CUG2-induced EGFR upregulation confers doxorubicin resistance to lung (cancer) cells through Stat1-HDAC4 signaling.

Electronic supplementary material The online version of this article (doi:10.1007/s13402-017-0343-7) contains supplementary material, which is available to authorized users.

✉ Young-Hwa Chung
younghc@pusan.ac.kr

[1] BK21+, Department of Cogno-Mechatronics Engineering, Pusan National University, Busan 46241, Republic of Korea

[2] Department of Nanoenergy Engineering, Pusan National University, Busan 46241, Republic of Korea

[3] Department of Optics & Mechatronics Engineering, Convergence Research Center of 3D Laser-Aided Innovative Manufacturing Technology, Pusan National University, Busan 46241, Republic of Korea

[4] Department of Biology, Faculty of Science, Thaksin University, Phatthalung 93210, Thailand

[5] Department of Biological Sciences, Dong-A University, Busan 49315, Republic of Korea

[6] Department of Toxicology, University Medical Center, 55131 Mainz, Germany

[7] Department of Biochemistry & Molecular Biology, Cumming School of Medicine, University of Calgary, Calgary T2N4N1, Canada

Keywords CUG2 · EGFR · Stat1 · HDAC4 · Drug resistance

1 Introduction

The cancer upregulated gene 2 (CUG2) has been identified as a candidate oncogene that is commonly upregulated in various cancers, including ovarian, liver, colon and lung cancer, and has been found to play a crucial role in tumorigenesis [1]. The *CUG2* gene maps to chromosome 6q22.32, spans ~8.5 kb, has a three-exon structure and encodes a 88-amino acid polypeptide [1]. Others have identified CUG2 as a new centromeric component that is required for proper kinetochore functioning during cell division [2, 3]. The oncogenic effect of CUG2 was found to be similar to that of mutant Ras in a NIH3T3 transplant model [1]. Whereas CUG2 overexpression activates Ras and MAPKs, including p38 MAPK, which facilitates oncolytic retroviral replication [4], it has also been found that CUG2 may confer resistance to oncolytic vesicular stomatitis virus infection [5] and induce cell migration and anti-cancer drug resistance through activation of Stat1 [6]. Additional studies have revealed that CUG2 may induce epithelial-mesenchymal transition (EMT) through TGF-β signaling and that crosstalk between Sp1 and Smad2/3 mediated by CUG2 or TGF-β may play a crucial role during EMT [7].

The epidermal growth factor receptor (EGFR) belongs to the ErbB family of proteins, and consists of an extracellular ligand-binding domain, a transmembrane domain and an intracellular tyrosine kinase domain which is responsible for its signal transducing capacity [8, 9]. EGFR-mediated signal transduction involves the Ras/MAPK and Src-Stat3 cascades as well as protein kinase C activation, all of which lead to increased cell proliferation, apoptosis inhibition and metastasis induction [9, 10]. EGFR overexpression has frequently been found in various cancers, including lung, gastric and colorectal cancer [11–13]. In addition, EGFR tyrosine kinase inhibitors, such as gefitinib and erlotinib, have been used for the treatment of non-small cell lung cancers with activating *EGFR* mutations [14, 15]. Although these inhibitors have been found to result in impressive clinical improvements, ultimately the patients may develop drug resistance due to mutations in the EGFR tyrosine kinase domain [16–18]. Also, anti-EGFR antibodies have been used to treat metastatic colorectal cancer patients without Ras mutations, as well as head and neck squamous cell carcinomas and others [19, 20].

Histone deacetylases (HDACs) play important roles in the maintenance and function of chromatin by regulating the acetylation status of histones [21, 22]. Recent data, however, indicate that HDACs may have additional roles in regulating the acetylation status of non-histone targets [23–25]. In particular, HDAC4, belonging to the class IIa family of HDACs, has been found to act as a regulator of transcription factors [23–25]. One study has shown that HDAC4 can bind to HIF-1α and that HDAC4 suppression can augment HIF-1α acetylation, leading to HIF-1α destabilization and down-regulation of HIF-1α-targeted gene transcription [23]. Another study has shown that HDAC4 may directly interact with Foxo1 and, by doing so, decrease its acetylation and upregulate its transcriptional activity [24]. Additional recent studies have shown that HDAC inhibition or suppression can activate Stat3 through its acetylation [26, 27]. HDAC4 overexpression has also been found to repress the activity of the p21 promoter, thereby promoting colon and gastric cancer cell growth [28, 29].

The aim of this study was to investigate the mechanism by which CUG2 confers doxorubicin resistance to cells. We found that CUG2 enhances EGFR expression, leading to upregulation of several antioxidant and multidrug resistance-related proteins, including MnSOD, Foxo1, Foxo4, MRP2 and BCRP. We also found that CUG2-induced EGFR upregulation was involved in Stat1 activation and increased HDAC4 expression. In addition, we found that Stat1 and HDAC4 silencing propelled doxorubicin-induced apoptosis, thus confirming the role of these molecules in conferring drug resistance to CUG2 overexpressing cells.

2 Materials and methods

2.1 Cell culture

Human lung cancer-derived A549 cells and immortalized human bronchial BEAS-2B cells were obtained from the ATCC (Manassas, VA, USA), and stably empty vector alone (A549-Vec; BEAS-Vec) or wild-type CUG2 expression vector (A549-CUG2; BEAS-CUG2) transfected cells were cultured in RPMI-1640 or 50% DMEM/50% F12 medium, respectively, at 37 °C in a 5% CO_2 humidified atmosphere. The different media were supplemented with 10% FBS, 1% penicillin, 1% streptomycin and 500 μg/ml G418 (Sigma-Aldrich, St. Louis, MO, USA).

2.2 Reagents and antibodies

Antibodies directed against total and phosphorylated Akt, ERK, JNK, p38 MAPK, Jak1, Tyk2 and Stat1, as well as antibodies directed against HDAC1, HDAC2, HDCA3, HDAC4, EGFR and cleaved PARP, were purchased from Cell Signaling Biotechnology (Danvers, MA, USA). Antibodies directed against β-actin, BCRP, MRP2, MnSOD, Foxo1 and Foxo4 were obtained from Santa Cruz Biotechnology (Santa Cruz, CA, USA). The protein kinase inhibitors wortmannin, PD98059, SP600125 and SB203580 were purchased from Calbiochem (San Diego, CA, USA). Trichostatin A (TSA) and doxorubicin were purchased from

Sigma-Aldrich. LY2109761 was purchased from Cayman Chemical (Ann Arbor, MI, USA) and IFN-α was purchased from R&D Systems (Minneapolis, MN, USA).

2.3 Western blotting and immunoprecipitation

Cells were harvested and lysed with lysis buffer containing 1% NP-40 and protease inhibitors (Sigma-Aldrich). For Western blotting, proteins from whole cell lysates were resolved through SDS-polyacrylamide gel electrophoresis (PAGE) in 10% or 12% gels, and transferred to nitrocellulose membranes. Primary antibodies were used at 1:1000 or 1:2000 dilutions, and secondary antibodies conjugated with horseradish peroxidase were used at a 1:2000 dilution, in 5% nonfat dry milk. For immunoprecipitation, cells were harvested after 48 h of transfection, and cell debris was removed by centrifugation at 10,000×*g* for 10 min at 4 °C. Cell lysates were precleared with 25 μl protein A/G agarose and incubated with a primary antibody and protein A/G agarose for 1 h at 4 °C. After three washes with lysis buffer, the precipitates were resolved by SDS-PAGE and analyzed by immunoblotting using appropriate antibodies. After washing, the membranes were evaluated using an enhanced chemiluminescence assay in conjunction with Image Quant LAS 4000 Mini (GE-Healthcare, Tokyo, Japan).

2.4 siRNA transfection

Before siRNA transfection, cells were trypsinized and cultured overnight to achieve 60–70% confluence. Next, EGFR, Stat1 or HDAC4 specific siRNAs (Bioneer, Daejeon, Korea) or a negative control siRNA (Bioneer) were mixed with Lipofectamine 2000 after which the cells were incubated with the transfection mixture for 6 h, rinsed with medium containing 10% FBS, and incubated for 48 h at 37 °C before harvesting.

2.5 Immunofluorescence assay

For immunofluorescence, cells grown on cover slips were fixed with 4% paraformaldehyde for 15 min, permeabilized with cold acetone for 15 min, blocked with 10% goat serum for 30 min and treated with primary antibodies (1:100 dilution) for 30 min at room temperature. After incubation, the cells were washed extensively with PBS, incubated with Alexa Fluor 418-conjugated goat anti-mouse or donkey anti-rabbit antibody (1:500 dilution; Molecular Probes, Eugene, OR, USA) in PBS for 30 min at room temperature and washed three times with PBS. For nuclear staining, the cells were incubated with DAPI for 5 min in the dark and washed three times with PBS. The coverslips with stained cells were mounted on slides with PBS containing 10% glycerol and imaged using fluorescence microscopy.

2.6 RT-PCR assay

Total RNA was extracted from cells using a RNeasy mini kit (Qiagen, Valencia, CA, USA) in accordance with the manufacturer's instructions. Next, 3 μg total RNA was converted to cDNA using Superscript II reverse transcriptase (Invitrogen, Carlsbad, CA, USA) and, after dilution, an optimized number of PCR cycles was performed using the following primers: human *Multidrug Resistance associated protein (MRP)2*, sense: 5′-ACA GAG GCT GGT GGC AAC C-3′ and anti-sense: 5′-ACC ATT ACC TTG TCA CTG TCC-3′; *Breast Cancer Resistance Protein* (*BCRP)*, sense: 5′-GAT CAC AGT CTT CAA GGA GAT C-3′ and anti-sense: 5′-CAG TCC CAG TAC GAC TGT GAC A-3′. *β-Actin* mRNA was used as an internal standard. After amplification, the products were subjected to electrophoresis in 2.0% agarose gels and stained with ethidium bromide.

2.7 Reactive oxygen species (ROS) measurement

Intracellular ROS levels were determined using the oxidative-sensitive fluorescence dye 2′,7′-dichlorodihydrofluorescein diacetate (DCF; Molecular Probes, Eugene, OR, USA). After treatment of the cells with 20 μM DCF for 30 min they were evaluated using a fluorescence microscope (Carl Zeiss; Axio-D1, Oberkochen, Germany).

2.8 Generation of a capacitance biosensor platform

Capacitance biosensors were generated using standard photolithography and a subsequent lift-off process as described elsewhere [30]. Briefly, a 1.4 μm thick photoresist (PR, AZ5214) mold was first mounted on a glass substrate. Next, a 100 nm thick Au film was deposited on the mold substrate after depositing a 5 nm thick Cr adhesion layer using a thermal evaporation technique. After removing superfluous portions of the metal film in a sonication bath containing acetone, 6-channel parallel plate capacitors were obtained. After this, a 50 nm thick insulating silicon dioxide layer was deposited on the capacitive electrodes using a chemical vapor deposition process which was subsequently patterned using a buffered oxide etchant with a photolithographically defined PR etching mask. The distance and overlap length of the electrode pairs were 50 μm and 200 μm, respectively. Finally, an acrylic well (Lab-tek; Thermo Fisher Scientific, Pittsburgh, PA, USA) was attached to the sensor substrate with a polydimethylsiloxane (Dow Corning, Auburn, MI, USA) bonding layer to perform measurements in a liquid environment.

2.9 Capacitance measurement

Capacitance measurements were performed on cultured cells maintained in suspension in PBS. Following sterilization of the capacitance sensor in ethanol under UV radiation, 5×10^4 cells (250 μl cell suspension) and 25 nM anti-EGFR antibody were added to each well after which time-dependent capacitance was measured using an α-analyzer (Novocontrol Co. Montabaur, Germany) at a frequency of 5 kHz and 0.1 Vrms. The electrical connection between the capacitance sensor and the analyzer was maintained using a silver paste. Capacitance was recorded every 5 min for a total of 1–3 h with a single capacitance sensor, which was mounted on an optical microscope (Olympus PME, Tokyo, Japan).

2.10 Statistical analysis

Data are presented as means ± standard deviation (SD). One-way ANOVA or an unpaired *t*-test was performed in GraphPad Prism for statistical analysis. A p-value < 0.05 was considered to denote statistical significance.

3 Results

3.1 Increased EGFR expression mediated by CUG2 confers resistance to doxorubicin-induced apoptosis

Although we have previously reported that exogenous expression of CUG2 in mouse colon cancer cells may induce resistance to doxorubicin [6], the mechanism underlying this resistance has so far not been revealed. Here, we first examined whether exogenous CUG2 overexpressing human lung cancer-derived A549 cells (A549-CUG2) exhibit doxorubicin resistance similar to that previously observed in mouse colon cancer cells. Indeed, we found that A549-CUG2, as well as immortalized human bronchial BEAS-CUG2 cells, showed resistance to doxorubicin, including loss of PARP cleavage, whereas control A549-Vec and BEAS-Vec cells were sensitive to this drug (Fig. 1a and Supplementary Fig. 1A). We next asked whether exogenous CUG2 overexpression in A549-CUG2 and BEAS-CUG2 cells might increase the respective EGFR protein expression levels. Using Western blotting, we found that A549-CUG2 and BEAS-CUG2 cells indeed showed increased EGFR expression levels compared to A549-Vec and BEAS-Vec cells, respectively (Fig. 1b and Supplementary Fig. 1B). Subsequent immunofluorescence microscopy confirmed CUG2-induced EGFR expression upregulation in A549 and BEAS-2B cells (Fig. 1c and Supplementary Fig. 1C). CUG2-induced EGFR upregulation was further assessed with a capacitance sensor using an anti-EGFR antibody, which can detect capacitance changes elicited by interactions between EGFR and EGF on the cell surface [30]. By doing so, we found a 2-fold increase in capacitance in A549-CUG2 cells compared to A549-Vec cells (Fig. 1d).

Upon EGFR siRNA concentration optimization, we found that 500 nM EGFR siRNA efficiently reduced EGFR expression (Fig. 1e). A siRNA-induced suppression of EGFR expression on the cell surface could subsequently be confirmed by capacitance measurement (Fig. 1f). Using A549-CUG2 cells treated with EGFR siRNA (500 nM), we finally asked whether the CUG2-mediated resistance to doxorubicin could be attributed to EGFR overexpression. We found that EGFR silencing in A549-CUG2 and BEAS-CUG2 cells led to doxorubicin-induced apoptosis, which was confirmed by the detection of cleaved PARP, a substrate of active caspase-3 and caspase-7 (Fig. 1g and Supplementary Fig. 1D). These results indicate that CUG2-mediated EGFR upregulation is involved in doxorubicin resistance.

3.2 CUG2-mediated EGFR upregulation leads to increased expression of antioxidant and multidrug resistance proteins and to a decrease in doxorubicin-induced ROS

Next, we explored the mechanism underlying doxorubicin resistance induced by CUG2. We found that in A549-Vec and BEAS-Vec cells, doxorubicin treatment produced ROS in a dose-dependent manner, whereas in A549-CUG2 and BEAS-CUG2 cells this treatment, even at the highest concentrations tested (5 and 0.5 μg/ml, respectively), failed to generate ROS (Fig. 2a and Supplementary Fig. 2A). We also found that the expression of antioxidant proteins, such as MnSOD, Foxo1 and Foxo4, was higher in A549-CUG2 and BEAS-CUG2 cells than in A549-Vec and BEAS-Vec cells, respectively (Fig. 2b and Supplementary Fig. 2B). In addition, we found that A549-CUG2 cells showed an increased expression of multidrug resistance (MDR) genes, such as *MRP2* and *BCRP*, compared to the control A549-Vec cells (Fig. 2c). These results suggest that CUG2 overexpression reduces ROS production and upregulation of several antioxidant proteins and MDR genes. Based on these results, we hypothesized that EGFR may play a role in the decrease of doxorubicin-mediated ROS production in CUG2 overexpressing cells. To test this hypothesis, we suppressed EGFR expression in A549-CUG2 and BEAS-CUG2 cells using siRNA and, by doing so, observed reduced MnSOD, Foxo1 and Foxo4 protein levels compared to those in cells treated with control siRNA (Fig. 2d and Supplementary Fig. 2C). These reduced protein levels resulted in higher ROS concentrations (Fig. 2e and Supplementary Fig. 2D). EGFR silencing also decreased the MRP2 and BCRP mRNA and protein levels compared to those of control siRNA treated cells (Fig. 2f and Supplementary Fig. 2C),

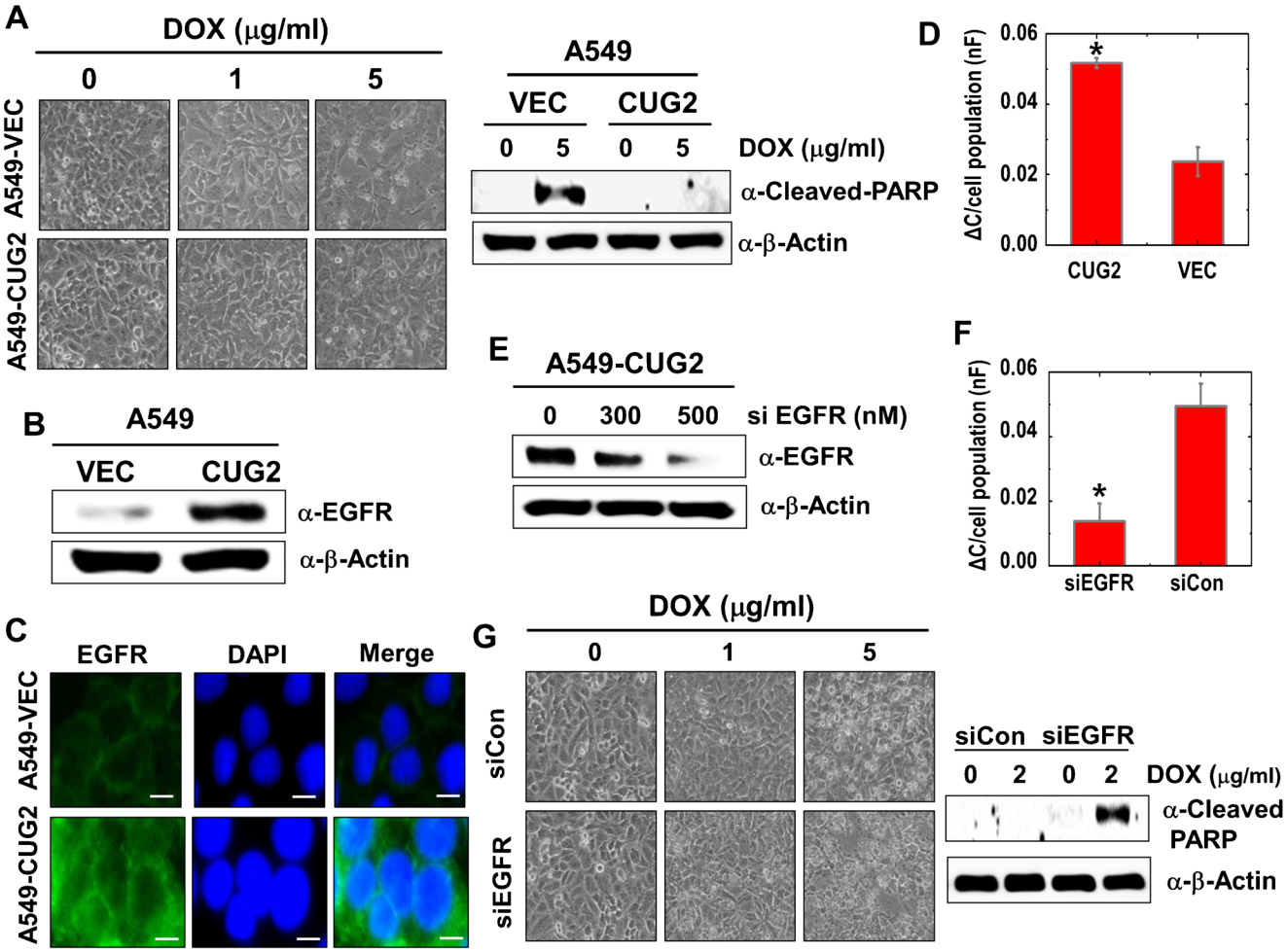

Fig. 1 EGFR suppression sensitizes A549-CUG2 cells to doxorubicin-induced apoptosis. **a** A549-Vec and A549-CUG2 cells were treated with doxorubicin (DOX; 0, 1 and 5 μg/ml) after which cell morphologies were monitored by light microscopy for 48 h. Cell lysates were analyzed by Western blotting using an antibody directed against cleaved PARP to detect apoptosis. **b** EGFR expression in A549-Vec and A549-CUG2 cells assessed by Western blotting using an anti-EGFR antibody. **c** EGFR expression assessed by immunofluorescence using Alexa Fluor 488-conjugated goat anti-rabbit IgG. For nuclear staining DAPI was used. The scale bar indicates 10 μm. **d** A549-Vec and A549-CUG2 cells were seeded into capacitance biosensor platform wells. Following the addition of an anti-EGFR antibody (25 nM) the capacitance in each well was measured. The data shown are the mean values of three independent experiments and the error bars indicate SD. (* denotes $p < 0.01$ for the comparison between CUG2 and Vec). **e** A549-CUG2 cells were treated with EGFR siRNA (300 and 500 nM) or control siRNA and the expression of EGFR was assessed by Western blotting using an anti-EGFR antibody. **f** A549-CUG2 cells were treated with EGFR siRNA (500 nM) or control siRNA for 48 h after which the cells were seeded into capacitance biosensor platform wells. Following the addition of an anti-EGFR antibody (25 nM) the capacitance in each well was measured. The data shown are the mean values of three independent experiments and the error bars indicate SD. (* denotes $p < 0.01$ for the comparison between EGFR siRNA and control siRNA). **g** A549-CUG2 cells were treated with EGFR siRNA (500 nM) or control siRNA in the absence or presence of doxorubicin (DOX; 1 and 5 μg/ml) after which cell morphologies were monitored by light microscopy for 48 h. Cell lysates were analyzed by Western blotting using an antibody directed against cleaved PARP to detect apoptosis

indicating that EGFR-mediated signaling controls ROS concentrations through the upregulation of antioxidant and multidrug resistance proteins.

3.3 CUG2-mediated EGFR upregulation leads to increased Akt, ERK, JNK and p38 MAPK-dependent Stat1 activation

Based on our previous work showing that Stat1 plays a role in doxorubicin resistance [6], we asked whether EGFR signaling might affect Stat1 activation. Similar to what we previously observed in murine colon cancer cells, we found that exogenous CUG2 overexpression resulted in an enhanced Stat1 phosphorylation in A549 and BEAS-2B cells (Fig. 3a and Supplementary Fig. 3A), whereas EGFR suppression resulted in a reduced Stat1 phosphorylation in these cells (Fig. 3b and Supplementary Fig. 3B). Using immunofluorescence microscopy, we found a predominant cytoplasmic localization of Stat1 in EGFR siRNA-treated A549-CUG2 cells and a predominant nuclear localization of Stat1 in control siRNA-treated A549-CUG2 cells (Fig.

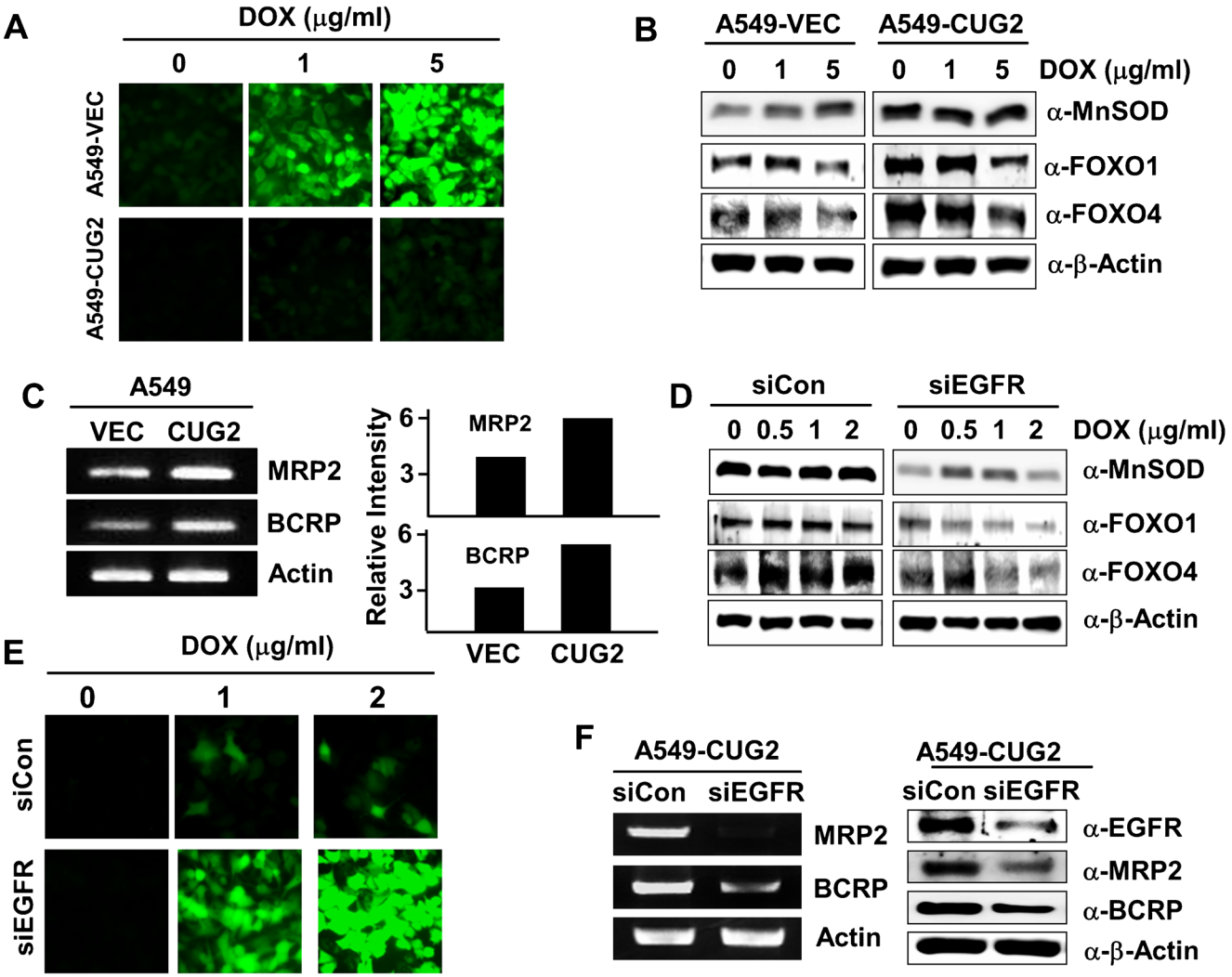

Fig. 2 Doxorubicin-induced ROS is alleviated by CUG2-mediated up-regulation of antioxidant and multidrug resistance proteins. **a**, **b** A549-Vec and A549-CUG2 cells were treated with doxorubicin (DOX; 0, 1 and 5 μg/ml), and the amount of ROS was measured by fluorescence microscopy 30 min after the addition of 20 μM DCF to the cells. The cells were harvested and lysed 48 h post-treatment and MnSOD, Foxo1 and Foxo4 expression was assessed by Western blotting using the corresponding antibodies. **c** Total RNA was isolated from A549-Vec and A549-CUG2 cells and subjected to RT-PCR. Transcription of *MRP2* and *BCRP* was determined after optimization of the PCR conditions. mRNA ratios of each MDR-related gene were determined relative to *β-actin* following band intensity measurements using Multi Gauge Version 2.1 (Fuji, Tokyo, Japan) software. **d**, **e**, **f** A549-CUG2 cells were treated with doxorubicin (DOX; 0, 0.5, 1 and 2 μg/ml) and subsequently incubated with EGFR siRNA or control siRNA for 48 h. ROS production was measured by fluorescence microscopy 30 min after the addition of 20 μM DCF to the cells. MnSOD, MRP2, BCRP, Foxo1 and Foxo4 expression was assessed 48 h post-transfection by Western blotting using the corresponding antibodies. Also total RNA was isolated 48 h post-transfection and analyzed by RT-PCR. *MRP2* and *BCRP* transcription was determined after optimization of the PCR conditions

3c). These results indicate that CUG2-mediated activation of Stat1 may be attributed to EGFR signaling. Next, we asked how EGFR signaling may lead to Stat1 activation. Recently, we reported that CUG2 may increase Akt, ERK, JNK and p38 MAPK phosphorylation [7]. Since these protein kinases may act as potential signaling molecules downstream of EGFR, we asked which of these serves as a direct target of EGFR signaling. To answer this question, A549-CUG2 cells were treated with EGFR siRNA after which the phosphorylation status of the respective protein kinases was examined. We found that Akt, ERK and JNK phosphorylation was decreased, whereas p38 MAPK phosphorylation was not (Fig. 3b). This result indicates that upon exogenous CUG2 overexpression, Akt, ERK and JNK activation depends on EGFR signaling, whereas p38 MAPK activation is independent of EGFR signaling. To identify which protein kinase is responsible for the activation of Stat1 upon exogenous CUG2 overexpression, we treated the respective cells with Akt, ERK, JNK or p38 MAPK inhibitors and subsequently assessed their Stat1 phosphorylation status. We found that all the inhibitors tested decreased Stat1 phosphorylation (Fig. 3d and Supplementary Fig. 3C). Although p38 MAPK is not a direct target of EGFR signaling, it has been found that it

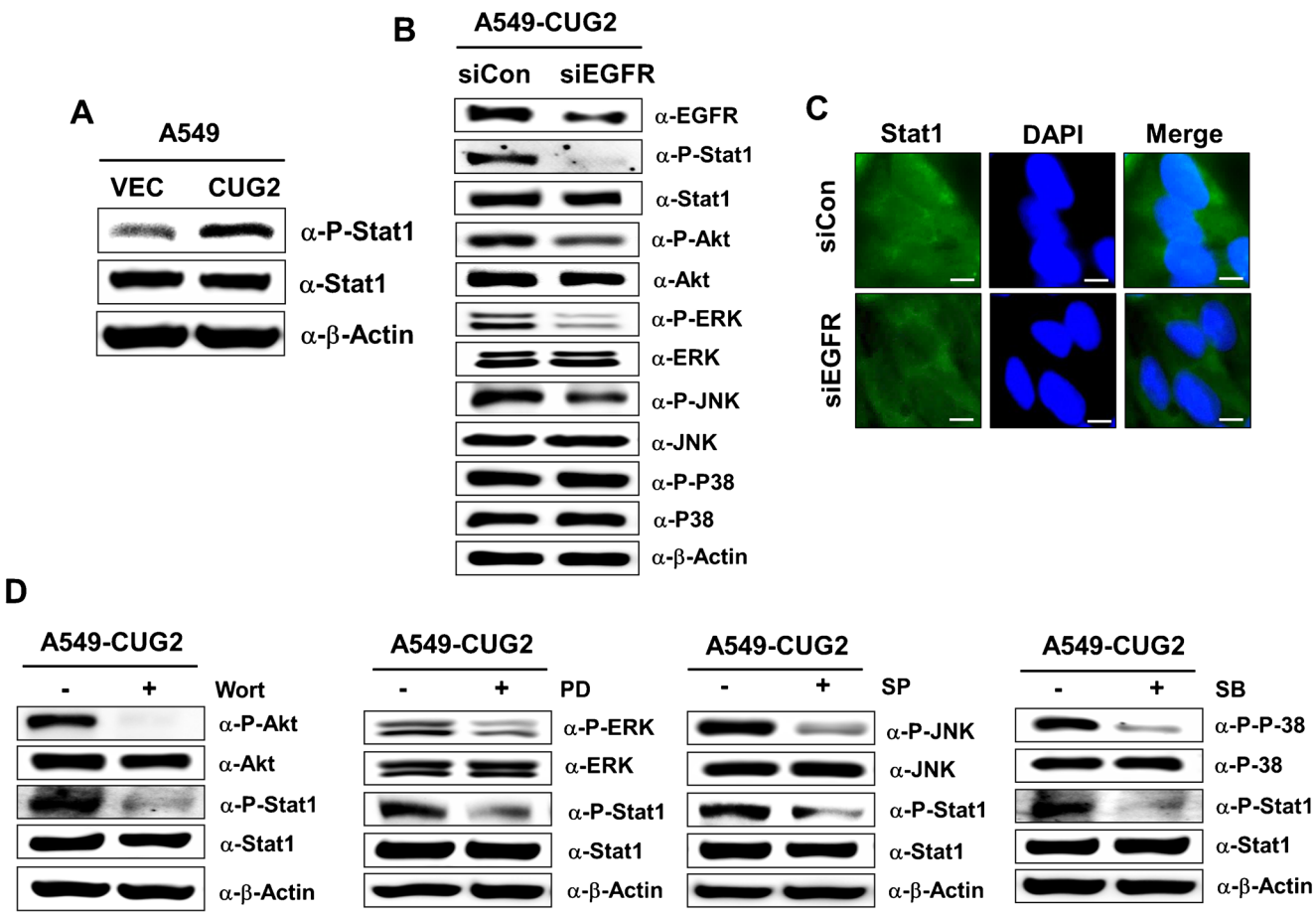

Fig. 3 Suppression of EGFR expression inhibits CUG2-induced activation of Stat1 signaling. **a** Cell lysates from A549-Vec and A549-CUG2 cells were used for the detection of total and phosphorylated Stat1 by Western blotting. **b** A549-CUG2 cells were treated with EGFR siRNA or control siRNA and the cells were lysed 48 h post-treatment. Total and phosphorylated Stat1, Akt, ERK, JNK and p38 MAPK expression was assessed by Western blotting using the corresponding antibodies. **c** Stat1 expression was assessed by immunofluorescence using Alexa Fluor 488-conjugated goat anti-rabbit IgG. For nuclear staining DAPI was used. The scale bar indicates 10 μm. **d** A549-CUG2 cells were treated with wortmannin (Wort; 10 μM), PD98059 (PD; 30 μM), SP600125 (SP; 20 μM) or SB203580 (SB; 20 μM) for 24 h. Total and phosphorylated Stat1, Akt, ERK, JNK and p38 MAPK expression was assessed by Western blotting using the corresponding antibodies

can be activated by CUG2 [7] and stimulate Stat1 phosphorylation. Taken together, these results indicate that Akt, ERK, JNK and p38 MAPK are involved in the EGFR-Stat1 signaling axis through CUG2 overexpression.

3.4 Upregulation of antioxidant and multidrug resistance proteins results from Stat1 activation through the CUG2-EGFR signaling axis

Based on our finding that EGFR signaling leads to Stat1 activation in CUG2 overexpressing cells, we next asked whether Stat1 plays a role in the doxorubicin resistance of these cells. We found that after siRNA-mediated Stat1 silencing the levels of several antioxidant proteins, including MnSOD, Foxo1 and Foxo4, were decreased, whereas the EGFR expression levels remained unchanged (Fig. 4a), indicating that these antioxidant proteins, but not EGFR, are directly related to Stat1 activation. Additionally, we found that Stat1 silencing also led to reduced Akt, ERK, JNK and p38 MAPK activation (Fig. 4b), suggesting crosstalk between Stat1 and these protein kinases. Interestingly, we found that siRNA-mediated Stat1 silencing led to decreased MRP2 protein levels, but not of BCRP (Fig. 4a), suggesting that MRP2 plays a more important role in the doxorubicin resistance of these cells than BCRP. Furthermore, we found that higher ROS concentrations were generated upon siRNA-mediated Stat1 silencing than upon control siRNA treatment (Fig. 4c), leading to induction of apoptosis as demonstrated by the detection of cleaved PARP (Fig. 4d). These results indicate that Stat1 activation induced by the CUG2-EGFR signaling axis plays a crucial role in the acquisition of doxorubicin resistance.

3.5 Increased Stat1 acetylation sensitizes lung (cancer) cells to doxorubicin-induced apoptosis

Since it has been found that Stat1 activity may be regulated not only by phosphorylation but also by acetylation [31, 32], we

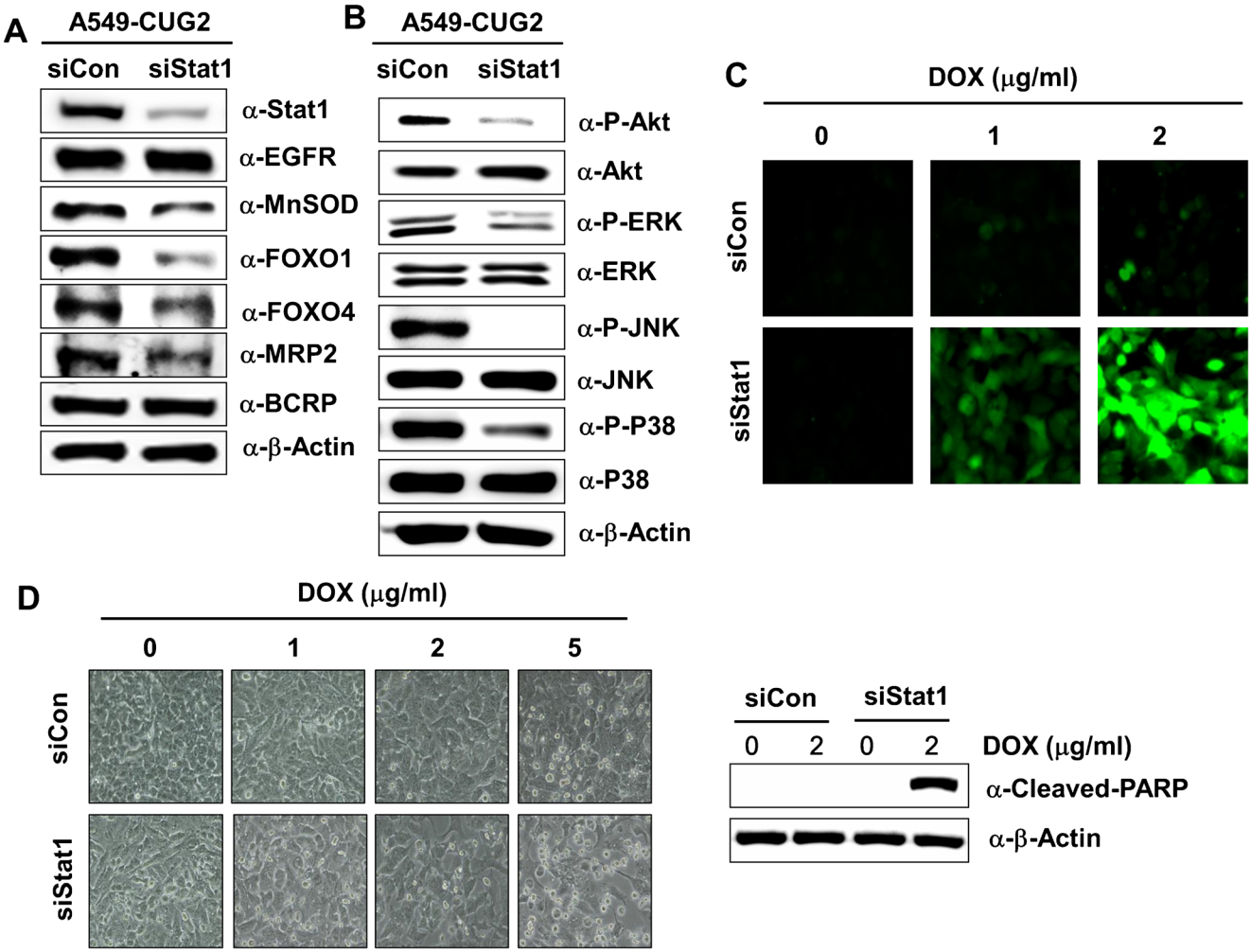

Fig. 4 Suppression of Stat1 sensitizes A549-CUG2 cells to doxorubicin-induced apoptosis. **a**, **b** A549-CUG2 cells were transfected with Stat1 siRNA (500 nM) or control siRNA and lysed 48 h post-treatment. Total and phosphorylated Stat1, EGFR, MnSOD, Foxo1, Foxo4, MRP2, BCRP, Akt, ERK, JNK and p38 MAPK expression were assessed by Western blotting using the corresponding antibodies. **c** A549-CUG2 cells were treated with doxorubicin (DOX; 0, 1 and 2 μg/ml) and subsequently incubated with Stat1 siRNA for 48 h. ROS production was measured by fluorescence microscopy 30 mi after the addition of 20 μM DCF to the cells. **d** A549-CUG2 cells were transfected with Stat1 siRNA or control siRNA in the presence of doxorubicin (DOX; 1, 2 and 5 μg/ml). Cell morphologies were monitored by light microscopy for 48 h. Next, cell lysates were analyzed by Western blotting using an antibody against cleaved PARP to detect apoptosis

applied TSA, a histone deacetylase inhibitor, to A549-CUG2 and BEAS-CUG2 cells. By doing so, we found that TSA treatment reduced Stat1 phosphorylation in these cells in a dose-dependent manner (Fig. 5a and Supplementary Fig. 4A). To assess whether TSA enhances Stat1 acetylation, we set out to immunoprecipitate Stat1 after TSA treatment. We found that in A549-Vec cells Stat1 exhibited lower phosphorylation and higher acetylation levels, whereas in A549-CUG2 cells Stat1 exhibited higher phosphorylation and lower acetylation levels (Fig. 5b). In addition, we found that IFN-α treatment induced translocation of Stat1 from cytoplasm to nucleus, which could be blocked by TSA treatment (Fig. 5c). Additionally, TSA treatment was found to significantly reduce the MRP2 expression level, whereas it only mildly reduced the expression levels of BCRP, MnSOD, Foxo1 and Foxo4 (Fig. 5a). As a consequence, we found that TSA treatment reduced the threshold for doxorubicin resistance, leading to apoptosis (Fig. 5d and Supplementary Fig. 4B). These results suggest that TSA-mediated acetylation leads to a less active form of Stat1, which fails to prevent A549-CUG2 and BEAS-CUG2 cells from undergoing doxorubicin-induced apoptosis.

3.6 CUG2-mediated enhancement of HDAC4 expression confers doxorubicin resistance through the EGFR-Stat1 signaling axis

Since we found that histone acetylation inhibitor (TSA) treatment affected Stat1 activation, we asked whether A549-CUG2 and A549-Vec cells express particular members of the HDAC family of proteins. We found that the expression levels of the class I HDACs, i.e., HDAC1, HDAC2 and HDAC3, were similar in both cell types (Fig. 6a). In contrast,

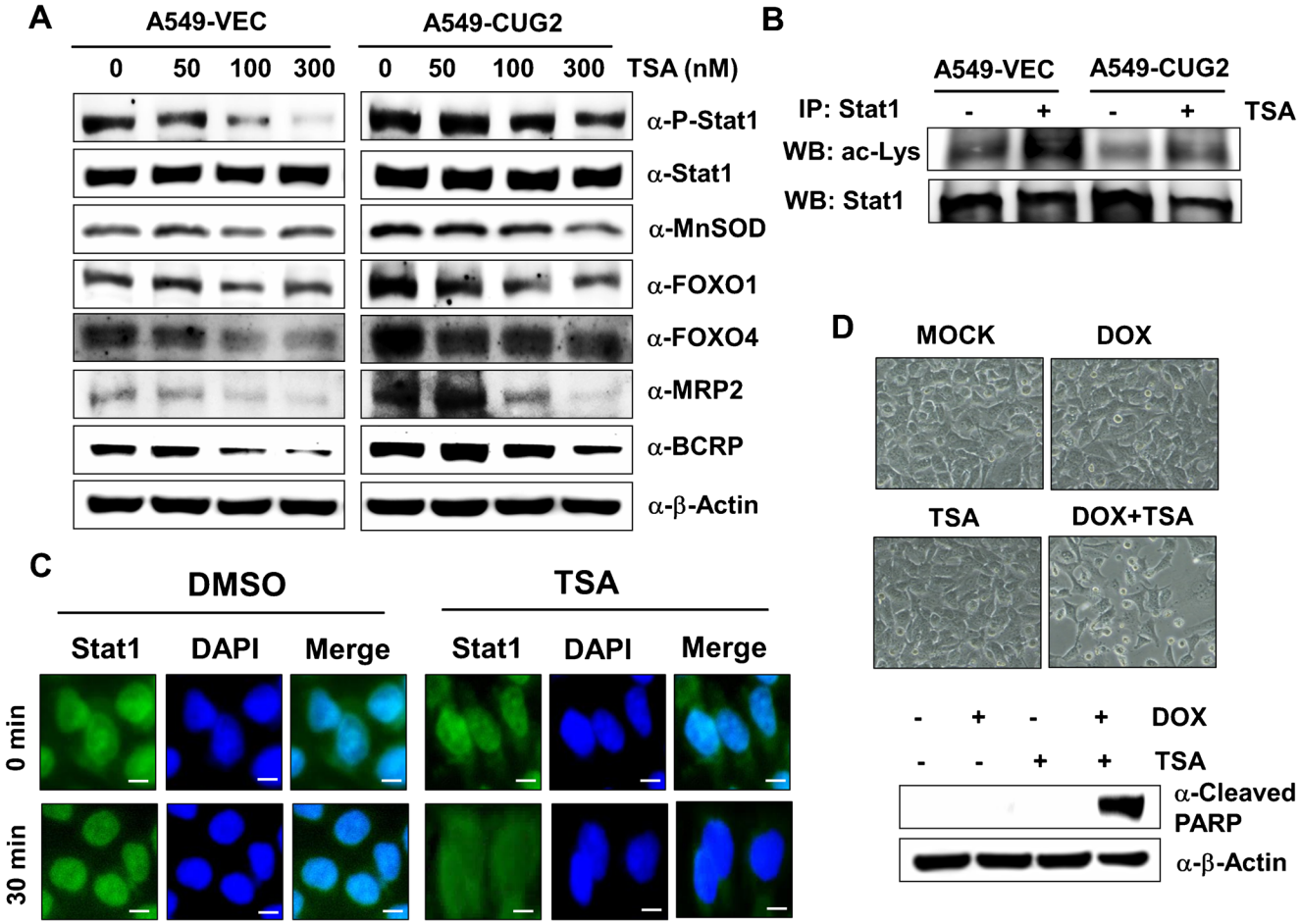

Fig. 5 Inhibition of HDACs with TSA reduces Stat1 activation, leading to doxorubicin-induced apoptosis. **a** A549-Vec and A549-CUG2 cells were treated with TSA (0, 50, 100 and 300 nM) for 24 h. Next, phospho-Stat1, Stat1, MRP2, BCRP, MnSOD, Foxo1 and Foxo4 expression was assessed by Western blotting using the corresponding antibodies. **b** A549-Vec and A549-CUG2 cells were treated with TSA (100 nM) for 24 h. Next, cell lysates were subjected to immunoprecipitation (IP) using an anti-Stat1 antibody for 1 h, followed by Western blotting using an antibody directed against acetylated lysine. **c** A549-CUG2 cells were transfected with a Stat1-GFP vector (1 μg) for 48 h, treated with IFN-α (100 units) in the absence or presence of TSA (100 nM) and evaluated by fluorescence microscopy. For nuclear staining, DAPI was used. The scale bar indicates 10 μm. **d** A549-CUG2 cells were treated with TSA (100 nM) in the absence or presence of doxorubicin (DOX; 2 μg/ml) and cell morphologies were monitored using light microscopy for 48 h. Next, cell lysates were analyzed by Western blotting using an antibody directed against cleaved PARP to detect apoptosis

we found that the class II HDAC4 expression level was significantly increased in A549-CUG2 cells compared to A549-Vec cells (Fig. 6a). In addition, we found that the HDAC1 and HDAC4 expression levels in BEAS-CUG2 cells were increased compared to those in BEAS-Vec cells, whereas the HDAC2 and HDAC3 expression levels were similar in both cell lines (Supplementary Fig. 5A). To directly determine whether elevated HDAC4 expression is related to doxorubicin resistance, we suppressed HDAC4 expression using siRNA. By doing so, we found that HDAC4 silencing resulted in decreased EGFR and phospho-Stat1 protein levels (Fig. 6b and Supplementary Fig. 5B). The effectiveness of the HDAC4 siRNA treatment was confirmed by a predominant cytoplasmic localization of Stat1 and a decreased fluorescence intensity of EGFR compared to that in control siRNA treated cells (Fig. 6c). siRNA-mediated HDAC4 silencing also led to decreased levels of the antioxidant proteins Foxo1, Foxo4 and MnSOD in BEAS-CUG2 cells (Supplementary Fig. 5B) and, except MnSOD, in A549-CUG2 cells (Fig. 6b), which may be attributed to the concomitant decrease in EGFR expression. We also detected a higher ROS production in HDAC4 silenced A549-CUG2 and BEAS-CUG2 cells than in control siRNA-treated A549-CUG2 and BEAS-CUG2 cells (Fig. 6d and Supplementary Fig. 5C). As a consequence, we found that HDAC4 suppression conferred doxorubicin sensitivity to A549-CUG2 and BEAS-CUG2 cells, leading to apoptosis (Fig. 6e and Supplementary Fig. 5D). In addition, we found that EGFR silencing specifically decreased HDAC4 expression, but not HDAC1, HDAC2 or HDAC3 expression, in A549-CUG2 cells (Fig. 6f), while EGFR silencing reduced the expression of HDAC1 and HDC4, but not of HDAC2 and HDAC3, in BEAS-CUG2 cells (Supplementary Fig.

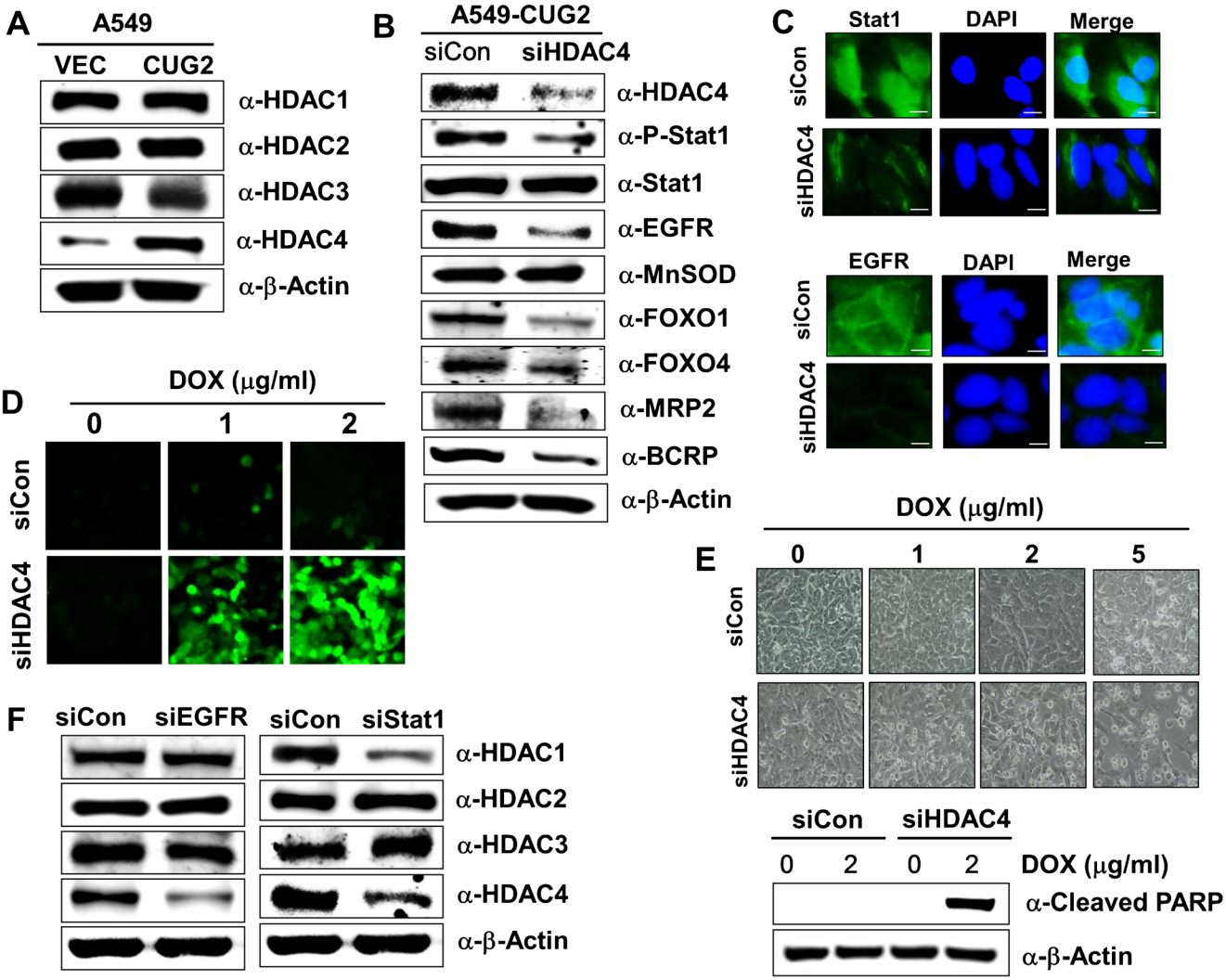

Fig. 6 HADC4 silencing sensitizes A549-CUG2 cells to doxorubicin-induced apoptosis. **a** HDAC1, 2, 3 and 4 expression in A549-Vec and A549-CUG2 cells was assessed by Western blotting using the corresponding antibodies. **b** A549-CUG2 cells were treated with HDAC4 siRNA (500 nM) or control siRNA and HDAC4, phospho-Stat1, Stat1, EGFR, MRP2, BCRP, MnSOD, Foxo1 and Foxo4 expression was assessed by Western blotting using the corresponding antibodies. **c** A549-CUG2 cells were treated with HDAC4 siRNA and Stat1 and EGFR expression was assessed by immunofluorescence using Alexa Fluor 488-conjugated goat anti-rabbit IgG. For nuclear staining DAPI was used. The scale bar indicates 10 μm. **d** A549-CUG2 cells were treated with HDAC4 siRNA or control siRNA for 48 h. ROS production was measured by fluorescence microscopy 30 min after the addition of 20 μM DCF to the cells. **e** A549-CUG2 cells were treated with HDAC4 siRNA or control siRNA in the absence or presence of doxorubicin (DOX; 0, 1, 2 and 5 μg/ml) and cell morphologies were monitored by light microscopy for 48 h. Cell lysates were analyzed by Western blotting using an antibody directed against cleaved PARP to detect apoptosis. **f** A549-CUG2 cells were treated with Stat1 siRNA (500 nM) or EGFR siRNA (500 nM) and HDAC1, 2, 3 and 4 expression was assessed by Western blotting using the corresponding antibodies

5E). Interestingly, we found that siRNA-mediated Stat1 knockdown led to reduced HDAC1 and HDAC4 protein levels, whereas it had no effect on the HDAC2 and HDAC3 protein levels in both cell lines (Fig. 6f and Supplementary Fig. 5E). Based on these results, we propose a model for an interplay between EGFR, Stat1 and HDAC4, which is depicted in Fig. 7. In summary, we conclude that our results indicate that CUG2-induced EGFR signaling upregulates HDAC4 expression in lung (cancer)-derived cells, resulting in resistance to doxorubicin-induced apoptosis.

4 Discussion

We found that CUG2-induced upregulation of EGFR leads to Stat1 activation, HDAC4 overexpression and doxorubicin resistance in lung (cancer)-derived cells. In a recent study, we have shown that CUG2 enhances TGF-β signaling, which is essential for EMT [7]. Others have shown that TGF-β can induce sorafenib resistance through receptor tyrosine kinases, including EGFR [33, 34]. Notably, a recent study has shown that TGF-β-mediated drug resistance may successfully be reversed by an EMT-reverting agent [35]. These observations

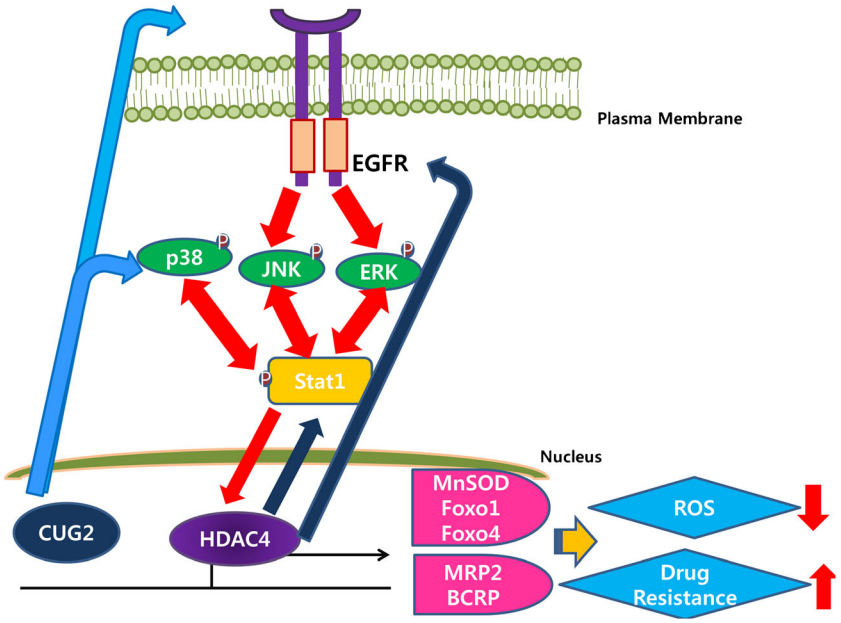

Fig. 7 Scheme of the proposed mechanism by which CUG2 confers resistance to doxorubicin. CUG2 overexpression upregulates EGFR signaling, leading to the activation of ERK and JNK. p38 MAPK is activated by CUG2 but not by EGFR signaling. Activated MAPKs activate Stat1, which in turn increases HDAC4 expression, but not EGFR expression. Conversely, increased HDAC4 expression induces Stat1 activation through EGFR upregulation. During signal transduction, increases in antioxidant proteins (MnSOD, Foxo1 and Foxo4) and multidrug resistance proteins (MRP2 and BCRP) result in a decrease in ROS level and an increase in drug resistance

led us to hypothesize that CUG2-mediated TGF-β signaling may be involved in EGFR upregulation. To test this hypothesis, we treated A549-Vec and BEAS-Vec cells with TGF-β. Conversely, we treated A549-CUG2 and BEAS-CUG2 cells with LY2157299, a TGFβRI kinase inhibitor, and subsequently assessed EGFR expression, Stat1 phosphorylation and HDAC4 expression. We found that TGF-β enhanced EGFR expression in A549-Vec and BEAS-Vec cells (Supplementary Fig. 6A). We also found that inhibition of TGF-β signaling decreased EGFR expression, leading to downregulation of Stat1 phosphorylation and HDAC4 expression, which is indicative for an interplay between EGFR and TGF-β signaling (Supplementary Fig. 6B). Others have reported that HDAC4 mediates deacetylation of SMAD4 and induces resistance to 5-fluorouracil, which underscores our hypothesis regarding the existence of a functional relationship between TGF-β and HDAC4 [36]. In addition, we found that combined treatment with LY2157299 and doxorubicin sensitized A549-CUG2 and BEAS-CUG2 cells to apoptosis (Supplementary Fig. 6C). The exact molecular mechanism by which CUG2-mediated TGF-β signaling upregulates EGFR expression remains, however, to be resolved and will be the subject of future studies.

We found that activation of Stat1 by CUG2-mediated EGFR signaling resulted in doxorubicin resistance. This observation is in conformity with that of others showing that constitutive activation of Stat1 confers resistance to doxorubicin to melanoma cells [37], and resistance to the platinum-based drug AMD473 to ovarian cancer cells [38]. Consequently, it was found that Stat1 suppression inhibited tumor growth and enhanced anti-cancer drug sensitivity [39, 40]. These changes were found to be accompanied by altered expression patterns of genes involved in processes such as glycolysis/gluconeogenesis, the citric acid cycle and oxidative phosphorylation. The most significant impact of Stat1 activation was found to be on the glycolysis/gluconeogenesis pathway, suggesting that Stat1-dependent regulation of metabolic pathways and energy consumption is associated with tumor growth and resistance to irradiation and drug treatment.

Stat1 activation can be modulated not only by phosphorylation but also by acetylation. Previous studies have shown that IFN-dependent signaling can be terminated by Stat1 acetylation and that HDAC activity is required for the accurate, Stat1-mediated recruitment of enhanceosomes to the promoter sites of Stat1-responsive genes [41–44]. Here, we found that HDAC inhibition or siRNA-mediated HDAC4 expression knockdown led to suppressed Stat1 activation. Previously, it has been shown that HDAC4 overexpression can lead to HIF-1α stabilization, Stat1 phosphorylation and an increase in Foxo1-mediated transcription, suggesting that HDAC4 may serve as a potential therapeutic target [23, 24]. A recent study also reported that HDAC4 may enhance colon cancer cell growth by reducing p21 transcription [29]. The notion that HDAC4 may play a positive role in cancer development is also supported by our observation that HDAC4 silencing sensitized cells to doxorubicin-induced apoptosis through the downregulation of Stat1 activity. Interestingly, we found that HDAC4 silencing reduced EGFR expression, although the

underlying mechanism remains to be resolved. Based on these results, we suggest that HDAC4 plays a positive role in the development of CUG2-induced (lung) cancer. Conversely, we found that EGFR suppression led to decreased HDAC4 expression levels. In addition, we found that Stat1 suppression led to decreased HDAC4 and HDAC1 levels but not to those of HDAC2 and HDAC3. In the future, we aim to delineate the mechanism by which EGFR and/or Stat1 suppression specifically decrease HDAC4 expression.

Acknowledgements This study was supported by the Basic Research Program of the National Research Foundation, funded by the Korean government (NRF-2014R A1A2053750), (MSIP) (NRF-2015R1A2A1A15056030), and (2015R1A5A7036513).

Author contributions S.K., R.N. J. and Y-H.C. conceived and designed the experiments. S.K., S.W.J., D.-M.S., C.K. and H.H.J. performed the experiments. Y.-H. H., K.K., B.S., C.S.K., S.S.K. and O.H.K contributed reagents and materials. S.K., R.N. J. and Y-H.C. wrote the paper.

Compliance with ethical standards

Conflicts of interest The authors declare no competing interest.

References

1. S. Lee, J. Gang, S.B. Jeon, S.H. Choo, B. Lee, Y.G. Kim, Y.S. Lee, J. Jung, S.Y. Song, S.S. Koh, Molecular cloning and functional analysis of a novel oncogene, cancer-upregulated gene 2 (CUG2). Biochem Biophys Res Commun **360**, 633–639 (2007)
2. T. Hori, M. Amano, A. Suzuki, C.B. Backer, J.P. Welburn, Y. Dong, B.F. McEwen, W.H. Shang, E. Suzuki, K. Okawa, I.M. Cheeseman, T. Fukagawa, CCAN makes multiple contacts with centromeric DNA to provide distinct pathways to the outer kinetochore. Cell **135**, 1039–1052 (2008)
3. H. Kim, M. Lee, S. Lee, B. Park, W. Koh, D.J. Lee, D.S. Lim, S. Lee, Cancer-upregulated gene 2 (CUG2), a new component of centromere complex, is required for kinetochore function. Mol Cell **27**, 697–701 (2009)
4. E.H. Park, I.R. Cho, R. Srisuttee, H.J. Min, M.J. Oh, Y.J. Jeong, B.H. Jhun, R.N. Johnston, S. Lee, S.S. Koh, Y.H. Chung, CUG2, a novel oncogene confers reoviral replication through Ras and p38 signaling pathway. Cancer Gene Ther **17**, 307–314 (2010)
5. W. Malilas, S.S. Koh, R. Srisuttee, W. Boonying, I.R. Cho, C.S. Jeong, R.N. Johnston, Y.H. Chung, Cancer upregulated gene 2, a novel oncogene, confers resistance to oncolytic vesicular stomatitis virus through STAT1-OASL2 signaling. Cancer Gene Ther **20**, 125–132 (2013)
6. W. Malilas, S.S. Koh, S. Kim, R. Srisuttee, I.R. Cho, J. Moon, H.S. Yoo, S. Oh, R.N. Johnston, Y.H. Chung, Cancer upregulated gene 2, a novel oncogene, enhances migration and drug resistance of colon cancer cells via STAT1 activation. Int J Oncol **43**, 1111–1116 (2013)
7. S. Kaowinn, J. Kim, J. Lee, D.H. Shin, C.D. Kang, D.K. Kim, S. Lee, M.K. Kang, S.S. Koh, S.J. Kim, Y.H. Chung, Cancer upregulated gene 2 induces epithelial-mesenchymal transition of human lung cancer cells via TGF-beta signaling. Oncotarget **8**, 5092–5110 (2017)
8. K.J. Wilson, J.L. Gilmore, J. Foley, M.A. Lemmon, D.J. Riese 2nd, Functional selectivity of EGF family peptide growth factors: Implications for cancer. Pharmacol Ther **122**, 1–8 (2009)
9. N. Normanno, A. De Luca, C. Bianco, L. Strizzi, M. Mancino, M.R. Maiello, A. Carotenuto, G. De Feo, F. Caponigro, D.S. Salomon, Epidermal growth factor receptor (EGFR) signaling in cancer. Gene **366**, 2–16 (2006)
10. M.A. Lemmon, J. Schlessinger, Cell signaling by receptor tyrosine kinases. Cell **141**, 1117–1134 (2010)
11. Y. Zhen, L. Guanghui, Z. Xiefu, Knockdown of EGFR inhibits growth and invasion of gastric cancer cells. Cancer Gene Ther **21**, 491–497 (2014)
12. Y. Yarden, M.X. Sliwkowski, Untangling the ErbB signalling network. Nat Rev Mol Cell Biol **2**, 127–137 (2001)
13. R.J. Silva-Oliveira, V.A. Silva, O. Martinho, A. Cruvinel-Carloni, M.E. Melendez, M.N. Rosa, F.E. de Paula, L. de Souza Viana, A.L. Carvalho, R.M. Reis, Cytotoxicity of allitinib, an irreversible anti-EGFR agent, in a large panel of human cancer-derived cell lines: KRAS mutation status as a predictive biomarker. Cell Oncol **39**, 253–263 (2016)
14. C. Gridelli, F. De Marinis, M. Di Maio, D. Cortinovis, F. Cappuzzo, T. Mok, Gefitinib as first-line treatment for patients with advanced non-small-cell lung cancer with activating epidermal growth factor receptor mutation: Review of the evidence. Lung Cancer **71**, 249–257 (2011)
15. M. Murphy, B. Stordal, Erlotinib or gefitinib for the treatment of relapsed platinum pretreated non-small cell lung cancer and ovarian cancer: A systematic review. Drug Resist Updat **14**, 177–190 (2011)
16. R. Bianco, T. Gelardi, V. Damiano, F. Ciardiello, G. Tortora, Rational bases for the development of EGFR inhibitors for cancer treatment. Int J Biochem Cell Biol **39**, 1416–1431 (2007)
17. S.N. Bichev, D.M. Marinova, Y.G. Slavova, A.S. Savov, Epidermal growth factor receptor mutations in east European non-small cell lung cancer patients. Cell Oncol **38**, 145–153 (2015)
18. Y.X. Bao, X.D. Zhao, H.B. Deng, C.L. Lu, Y. Guo, X. Lu, L.L. Deng, Schedule-dependent cytotoxicity of sunitinib and TRAIL in human non-small cell lung cancer cells with or without EGFR and KRAS mutations. Cell Oncol **39**, 343–352 (2016)
19. M.J. Sotelo, B. Garcia-Paredes, C. Aguado, J. Sastre, E. Diaz-Rubio, Role of cetuximab in first-line treatment of metastatic colorectal cancer. World J Gastroenterol **20**, 4208–4219 (2014)
20. J.E. Frampton, Cetuximab: A review of its use in squamous cell carcinoma of the head and neck. Drugs **70**, 1987–2010 (2010)
21. X.J. Yang, E. Seto, HATs and HDACs: From structure, function and regulation to novel strategies for therapy and prevention. Oncogene **26**, 5310–5318 (2007)
22. A. Ferraro, Altered primary chromatin structures and their implications in cancer development. Cell Oncol **39**, 195–210 (2016)
23. H. Geng, C.T. Harvey, J. Pittsenbarger, Q. Liu, T.M. Beer, C. Xue, D.Z. Qian, HDAC4 protein regulates HIF1α protein lysine acetylation and cancer cell response to hypoxia. J Biol Chem **286**, 38095–38102 (2011)
24. M.M. Mihaylova, D.S. Vasquez, K. Ravnskjaer, P.D. Denechaud, R.T. Yu, J.G. Alvarez, M. Downes, R.M. Evans, M. Montminy, R.J. Shaw, Class IIa histone deacetylases are hormone-activated regulators of FOXO and mammalian glucose homeostasis. Cell **145**, 607–621 (2011)
25. E.A. Stronach, A. Alfraidi, N. Rama, C. Datler, J.B. Studd, R. Agarwal, T.G. Guney, C. Gourley, B.T. Hennessy, G.B. Mills, A. Mai, R. Brown, R. Dina, H. Gabra, HDAC4-regulated STAT1 activation mediates platinum resistance in ovarian cancer. Cancer Res **71**, 4412–4422 (2011)
26. Y. Sun, Y.E. Chin, E. Weisiger, C. Malter, I. Tawara, T. Toubai, E. Gatza, P. Mascagni, C.A. Dinarello, P. Reddy, Cutting edge: Negative regulation of dendritic cells through acetylation of the nonhistone protein STAT-3. J Immunol **182**, 5899–5903 (2009)

27. Z.L. Yuan, Y.J. Guan, D. Chatterjee, Y.E. Chin, Stat3 dimerization regulated by reversible acetylation of a single lysine residue. Science **307**, 269–273 (2005)
28. Z.H. Kang, C.Y. Wang, W.L. Zhang, J.T. Zhang, C.H. Yuan, P.W. Zhao, Y.Y. Lin, S. Hong, C.Y. Li, L. Wang, Histone deacetylase HDAC4 promotes gastric cancer SGC-7901 cells progression via p21 repression. PLoS One **9**, e98894 (2014)
29. A.J. Wilson, D.S. Byun, S. Nasser, L.B. Murray, K. Ayyanar, D. Arango, M. Figueroa, A. Melnick, G.D. Kao, L.H. Augenlicht, J.M. Mariadason, HDAC4 promotes growth of colon cancer cells via repression of p21. Mol Biol Cell **19**, 4062–4075 (2008)
30. D.M. Shin, Y.C. Shin, J.H. Lee, T.H. Kim, D.W. Han, J.M. Kim, H.K. Kim, K. Kim, Y.H. Hwang, Highly sensitive detection of epidermal growth factor receptor expression levels using a capacitance sensor. Sensors Actuators B Chem **209**, 438–443 (2015)
31. O.H. Kramer, T. Heinzel, Phosphorylation-acetylation switch in the regulation of STAT1 signaling. Mol Cell Endocrinol **315**, 40–48 (2010)
32. S. Zhuang, Regulation of STAT signaling by acetylation. Cell Signal **25**, 1924–1931 (2013)
33. D. Zhao, B. Zhai, C. He, G. Tan, X. Jiang, S. Pan, X. Dong, Z. Wei, L. Ma, H. Qiao, H. Jiang, X. Sun, Upregulation of HIF-2alpha induced by sorafenib contributes to the resistance by activating the TGF-alpha/EGFR pathway in hepatocellular carcinoma cells. Cell Signal **26**, 1030–1039 (2014)
34. N. Ungerleider, C. Han, J. Zhang, L. Yao and T. Wu, TGFbeta signaling confers sorafenib resistance via induction of multiple RTKs in hepatocellular carcinoma cells. Mol Carcinog **56**, 1302-1311 (2017)
35. R. Kurimoto, S. Iwasawa, T. Ebata, T. Ishiwata, I. Sekine, Y. Tada, K. Tatsumi, S. Koide, A. Iwama, Y. Takiguchi, Drug resistance originating from a TGF-beta/FGF-2-driven epithelial-to-mesenchymal transition and its reversion in human lung adenocarcinoma cell lines harboring an EGFR mutation. Int J Oncol **48**, 1825–1836 (2016)
36. S.L. Yu, D.C. Lee, J.W. Son, C.G. Park, H.Y. Lee, J. Kang, Histone deacetylase 4 mediates SMAD family member 4 deacetylation and induces 5-fluorouracil resistance in breast cancer cells. Oncol Rep **30**, 1293–1300 (2013)
37. N.N. Khodarev, P. Roach, S.P. Pitroda, D.W. Golden, M. Bhayani, M.Y. Shao, T.E. Darga, M.G. Beveridge, R.F. Sood, H.G. Sutton, M.A. Beckett, H.J. Mauceri, M.C. Posner, R.R. Weichselbaum, STAT1 pathway mediates amplification of metastatic potential and resistance to therapy. PLoS One **4**, e5821 (2009)
38. D. Roberts, J. Schick, S. Conway, S. Biade, P.B. Laub, J.P. Stevenson, T.C. Hamilton, P.J. O'Dwyer, S.W. Johnson, Identification of genes associated with platinum drug sensitivity and resistance in human ovarian cancer cells. Br J Cancer **92**, 1149–1158 (2005)
39. M. Fryknas, S. Dhar, F. Oberg, L. Rickardson, M. Rydaker, H. Goransson, M. Gustafsson, U. Pettersson, P. Nygren, R. Larsson, A. Isaksson, STAT1 signaling is associated with acquired crossresistance to doxorubicin and radiation in myeloma cell lines. Int J Cancer **120**, 189–195 (2007)
40. L. Rickardson, M. Fryknas, S. Dhar, H. Lovborg, J. Gullbo, M. Rydaker, P. Nygren, M.G. Gustafsson, R. Larsson, A. Isaksson, Identification of molecular mechanisms for cellular drug resistance by combining drug activity and gene expression profiles. Br J Cancer **93**, 483–492 (2005)
41. H.M. Chang, M. Paulson, M. Holko, C.M. Rice, B.R. Williams, I. Marie, D.E. Levy, Induction of interferon-stimulated gene expression and antiviral responses require protein deacetylase activity. Proc Natl Acad Sci U S A **101**, 9578–9583 (2004)
42. L. Klampfer, J. Huang, L.A. Swaby, L. Augenlicht, Requirement of histone deacetylase activity for signaling by STAT1. J Biol Chem **279**, 30358–30368 (2004)
43. J. Vlasakova, Z. Novakova, L. Rossmeislova, M. Kahle, P. Hozak, Z. Hodny, Histone deacetylase inhibitors suppress IFNalpha-induced up-regulation of promyelocytic leukemia protein. Blood **109**, 1373–1380 (2007)
44. I. Nusinzon, C.M. Horvath, Interferon-stimulated transcription and innate antiviral immunity require deacetylase activity and histone deacetylase 1. Proc Natl Acad Sci U S A **100**, 14742–14747 (2003)